LES of steady spray flame and ignition sequences in aeronautical combustors

S. Pascaud[†,*], M. Boileau[†], L. Martinez[†], B. Cuenot[†] and T. Poinsot[‡]

[†] *CERFACS, Toulouse, France* [‡] *IMFT - CNRS, Toulouse, France*

Ground ignition and altitude re-ignition are critical issues for aeronautical gas turbine design. They are strongly influenced by the turbulent flow structure as well as the liquid fuel spray and its atomization. Turbulent mixing, evaporation and combustion that control the combustion process are complex unsteady phenomena coupling fluid mechanics, thermodynamics and chemistry. To better understand unsteady combustion in industrial burners, Large Eddy Simulation (LES) is a unique and powerful tool. Its potential has been widely demonstrated in the context of turbulent cold flows, and it has been recently applied to turbulent combustion. Its extension to two-phase turbulent combustion is a challenge but recent results confirm that it brings totally new insight into the physics of flames for both mean and unsteady aspects. In the present work, an Euler-Euler formulation of the two-phase flow equations is coupled with a sub-grid scale model and a turbulent combustion model. The obtained two-fluid model computes the conservation equations in each phase and the exchanges source terms for mass and heat transfer between gas and liquid. Thanks to the compressible form of the gas equations, flame/acoustics interactions are resolved. For application to complex geometries, unstructured meshes are used. With this numerical tool, turbulent two-phase flames are simulated in an industrial gas turbine. Some of the mechanisms involved in the steady spray flame are analysed and the partially premixed flame structure is detailed. Nevertheless, the capabilities of the LES technique for spray combustion are not limited to the stabilised spray flame. Unsteady complex phenomena such as ignition sequences give promising results : the unsteady behaviour of the reacting two-phase flow from the installation of a kernel to the possible propagation and stabilisation of the flame is computed and demonstrates the LES capabilities in such unsteady complex problems.

Context

The main part of the production of energy comes from combustion of liquid hydrocarbon fuels, because of their convenient way of storage and transport. Most of the current combustion chambers burn liquid fuel using injectors which atomise, generally at high pressures, the liquid jet or film in small droplets (typically $10 - 200\ \mu m$). Then, the fuel becomes gaseous and an inhomogeneous mixing of air and vaporised fuel is created. For reasons of simplicity, this first step of atomisation is supposed to be instantaneous and numerical tools for evaporation and gaseous combustion are applied to two-phase flow combustors. This allows to study the influence of the liquid phase on steady flames and ignition sequences.

The Large Eddy Simulations (LES) technique is used to understand unsteady phenomena occurring in turbulent spray combustion. Many proofs of the LES capabilities are available for gaseous combustion[1–6] but very few studies deal with the complex topic of LES for two-phase reacting flows.[7–10]

The modelling of the liquid phase in a LES solver is an important issue for which two classes of methods are available : the Euler framework (EF) and the Lagrange framework (LF). The LF[7] describes the liquid phase as a huge but finite number of droplets with their own trajectory, velocity, temperature and diameter while the EF,[11,12] with an opposite point of view, considers the liquid phase as a continuous field whose characteristics are determined through a set of conservation equations for the liquid volume fraction, the liquid phase velocity and temperature, and the first/second order moments of the size distribution. Several complex phenomena like droplet/droplet coalescence and collision or droplet/wall interaction are easier to model in a LF. However, the choice of the EF is justified for a parallel computation of an unsteady spray combustion in a realistic combustor by the following arguments :

Parallelism : LES in complex geometries needs high CPU time and requires parallel computing. However, the efficient implementation of LF on a parallel computer is a critical issue and implies good load balancing,[13] whereas EF is directly parallelised with the same algorithms as the gas phase.

Number of droplets : the LES technique is less dissipative than RANS methods. As a consequence, the number of Lagrangian droplets at each time step in each cell must be sufficient to provide a smooth and accurate continuous field of gaseous fuel. Because the fuel vapour distribution, directly produced by the discrete droplet evaporation source terms, controls the propagation of the front,[14,15] this is crucial for two-phase flame computations. Very limited experience on this question is available today but it is likely that combustion requires much more particles than usually done for dispersion or evaporation studies, leading to uncontrolled CPU costs.

[*] pascaud@cerfacs.fr

Size distribution : since the spray granulometry controls the flame regime, a droplet size distribution must be considered. LF is better on this question because it naturally discretises droplets with different sizes. However, recent studies demonstrate the EF capabilities to include polydispersed sprays.[16–18]
Inlet conditions : due to the atomisation complexity, the accurate determination of the spray characteristics is a critical issue. Even if LF calculates droplet trajectories with precision, very approximate injection conditions will lead to rough results. Close to the injector, the liquid spray is organised as dense blobs[19] and LF can not be applied to these high-loaded zones. As a contrary, EF is more compatible with the physics of liquid injection.

Numerical tool

The solver *AVBP*, developed at *CERFACS*, is a parallel fully compressible code which computes the turbulent reacting two-phase flows, on both structured and unstructured grids, for complex industrial applications such as ignition sequences or acoustic instabilities. Turbulent combustion modelling is ensured by the Dynamically Thickened Flame model,[20] using a thickening factor F and an efficacity function E to determine the flame front turbulent velocity.[21] Subgrid scale turbulent viscosity is defined by the WALE model,[22] derived from the classic Smagorinsky model. The Euler/Euler framework governing a turbulent reacting two-phase flow is composed, for each phase, of a set of conservative equations defined by Eq. (1) and Eq. (2) and solved with the same numerical approach.

$$\text{Carrier phase} \qquad \frac{\partial \overline{\mathbf{w}}}{\partial t} + \nabla \cdot \overline{\mathbf{F}} = \overline{\mathbf{s}} \tag{1}$$

$$\text{Dispersed phase} \qquad \frac{\partial \overline{\mathbf{w}}_l}{\partial t} + \nabla \cdot \overline{\mathbf{F}}_l = \overline{\mathbf{s}}_l \tag{2}$$

For the carrier phase, the vector of conservative variables is defined by Eq. (3) with ρ the density, (u_1, u_2, u_3) the velocity components, E_t the total non chemical energy and Y_k the fuel mass fractions. The flux tensor $\overline{\mathbf{F}}$ is composed of viscous, inviscid and subgrid scale components and $\overline{\mathbf{s}}$ is the source term defined by Eq. (4). Combustion terms are the reaction rate $\overline{\dot{\omega}}_k$ and the heat release $\overline{\dot{\omega}}_T$ modelled by an Arrhenius law.[23] Additional source terms representing exchanges between phases are the mass transfer $\overline{\Gamma}$, the momentum transfer $\overline{I_i}$ and the enthalpy transfer $\overline{\Pi}$.

$$\overline{\mathbf{w}} = (\overline{\rho}\tilde{u}_1, \overline{\rho}\tilde{u}_2, \overline{\rho}\tilde{u}_3, \overline{\rho}\tilde{E}_t, \overline{\rho}\tilde{Y}_k) \tag{3}$$

$$\overline{\mathbf{s}} = (\overline{I_1}, \overline{I_2}, \overline{I_3}, \frac{E}{F}\overline{\dot{\omega}}_T + \overline{I_i}\tilde{u}_i + \overline{\Pi} + \overline{\dot{\omega}}_{spark}, -\frac{E}{F}\overline{\dot{\omega}}_k + \overline{\Gamma}\delta_{kF}) \tag{4}$$

For the dispersed phase, the vector of conservative variables $\overline{\mathbf{w}}_l$ is defined by Eq. (5) with α_l the volume fraction, $(u_{1,l}, u_{2,l}, u_{3,l})$ the velocity components, $h_{s,l}$ the sensible enthalpy and n_l the droplet number density. The flux tensor $\overline{\mathbf{F}}_l$ is only composed of convective terms and the source term $\overline{\mathbf{s}}$ is defined by Eq. (6).

$$\overline{\mathbf{w}}_l = (\overline{\alpha_l}\overline{\rho_l}, \overline{\alpha_l}\overline{\rho_l}\tilde{u}_{1,l}, \overline{\alpha_l}\overline{\rho_l}\tilde{u}_{2,l}, \overline{\alpha_l}\overline{\rho_l}\tilde{u}_{3,l}, \overline{\alpha_l}\overline{\rho_l}\tilde{h}_{s,l}, \overline{n_l}) \tag{5}$$

$$\overline{\mathbf{s}}_l = (-\overline{\Gamma}, -\overline{I_1}, -\overline{I_2}, -\overline{I_3}, -\overline{\Pi}, 0) \tag{6}$$

The fully explicit finite volume solver *AVBP* uses a cell-vertex discretisation and a second order time and space Lax-Wendroff centred numerical scheme.[24] Characteristic boundary conditions NSCBC[25] are used.

Configuration

The computed configuration is a 3D sector of 22.5-degrees of an annular aeronautical gas turbine at atmospheric pressure. The kerosene liquid spray *LS* is located at the center of the main swirled inlet SI (Fig. 1). An annular series of small holes H are located around the inlet to lift the flame and protect the injector from high temperatures. Then, several holes on the upper and lower walls are divided in two parts. The first part of the combustor where combustion takes place is located between the injector and the primary jets PJ, which bring cold air to the flame. The second part called dilution zone is located between PJ and dilution jets DJ, that reduce and homogenise the outlet temperature to protect the turbine. The spark plug SP is located under the upper wall between two PJ (Fig. 2). The geometry (Fig. 3) also includes cooling films which protect upper and lower walls from the flame.
The inlet and outlet boundary conditions are characteristic with relaxation coefficients to reduce reflexion.[26] The SI imposed velocity field mimics the swirler influence. The other inlets are simple non-swirled jets. Non-slip conditions are used on the upper and lower walls while symmetry condition is used on the chamber sides. $15\ \mu m$-droplets are injected at the SI center through a specific condition which specifies a liquid volumic fraction $\alpha_l \simeq 10^{-3}$. The droplets at $288\ K$ are heated by the air at $525\ K$. The initial liquid velocity is equal to the gaseous velocity as the droplet Stokes number, based on the droplet relaxation time, is lower than one.

The unstructured mesh is composed of 400000 nodes and 2300000 tetrahedra. The explicit time step is $\Delta t \simeq 0.22\ \mu s$. The mesh is refined close to the inlets and in the combustion zone (Fig. 4).
The Arrhenius coefficients are fitted by a genetic algorithm[27] from a reduced chemistry[28] to the present one-step chemistry : $JP10 + 14\ O_2 \rightleftharpoons 10\ CO_2 + 8\ H_2O$ using criteria such as flame speed and thickness.

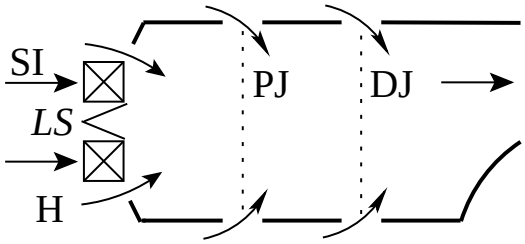

Fig. 1 Geometry sketch : side view

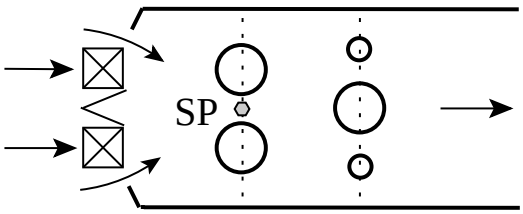

Fig. 2 Geometry sketch : top view

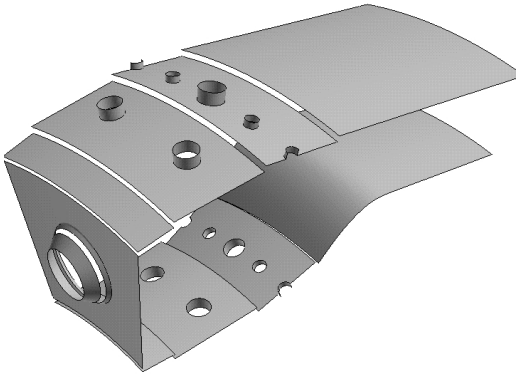

Fig. 3 Complex geometry

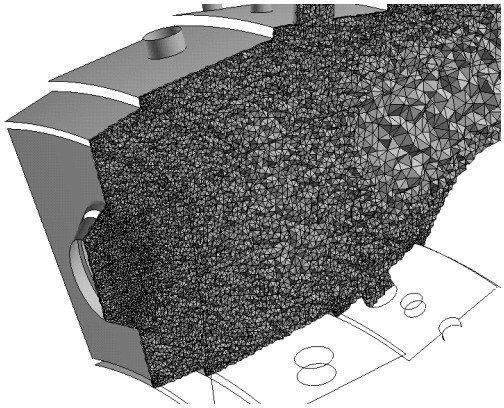

Fig. 4 Mesh refinement : central longitudinal view

Steady spray flame

Precessing Vortex Core

In its review on vortex breakdown, Lucca-Negro[29] classifies the hydrodynamic instabilities appearing in swirled flows. For high swirl numbers, the axial vortex breaks down at the stagnation point S and a spiral is created around a central recirculation zone CRZ (Fig. 5) : this vortex breakdown is the so-called precessing vortex core (PVC) existing in a large number of combustors.[30] The LES technique capture the vortex breakdown in the combustor and its frequency is evaluated with the backflow line on a transverse plane (Fig. 6) at six successive times marked with a number from 1 to 6 and separated by 0.5 ms. The turnover time is estimated at $\tau_{swirl} \simeq 3.5$ ms, corresponding to a frequency of $f_{PVC} \simeq 286$ Hz. Moreover, the three rotating motions of the SI, the whole PVC structure and the spiral winding turn in the same sense, as illustrated by the rotating arrows on Fig. 5.

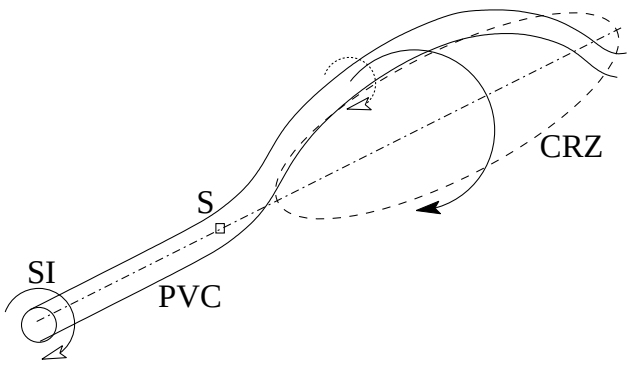

Fig. 5 Precessing Vortex Core

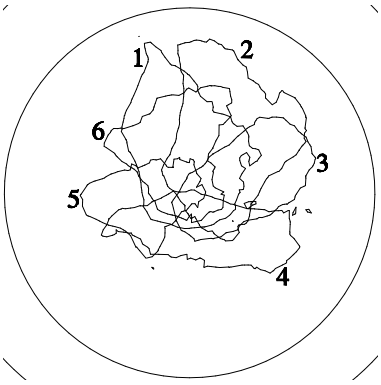

Fig. 6 Backflow line : transverse cut plane

Dispersion and evaporation

The $15\ \mu m$ droplets motion follows the carrier phase dynamics so that the CRZ of both zones are similar, as illustrated by both backflow lines on Fig. 7. Maintained by this CRZ, the droplets accumulate and the droplet number density, presented with the liquid volumic fraction field on Fig. 7, rises above its initial value. Increasing the residence time of these vaporising droplets, whose diameter field is presented on Fig. 8, makes the local equivalence ratio distribution reach values higher than 10. The heat transfer linked to the phase change leads to the reduction of the gaseous temperature, as shown by the isoline $T = 450\ K$ on Fig. 9, and an increase of the dispersed phase temperature. Thus, the CRZ, by trapping evaporating droplets, stabilise the vaporised fuel and the flame.

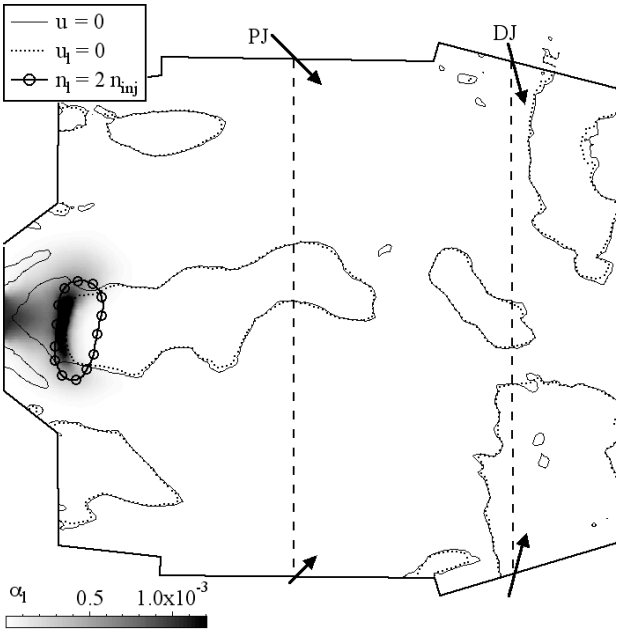

Fig. 7 Dispersion

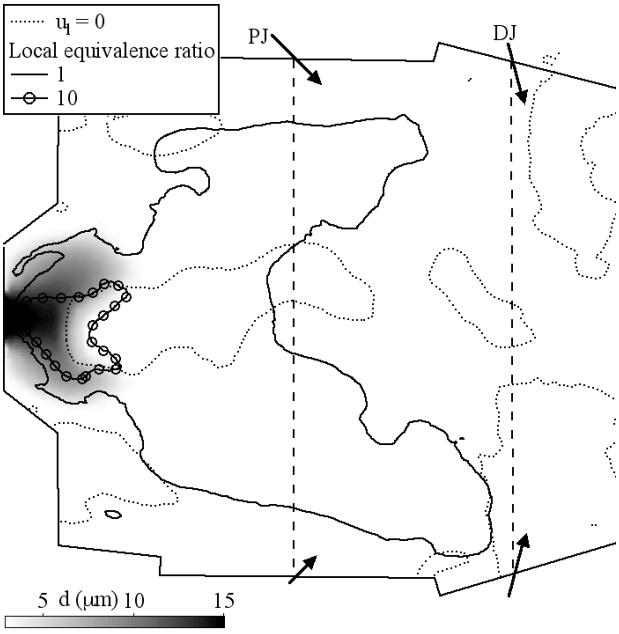

Fig. 8 Evaporation

Combustion

The flame front, illustrated on Fig. 9 by the heat release field, is influenced by both flow dynamics and evaporation rate. The main competitive phenomena for two-phase flame stabilisation are :

1. the air velocity must be low enough to match the turbulent flame velocity : the dynamics of the carrier phase (and in particular the CRZ) stabilise the flame front on a stable pocket of hot gases
2. zones where the local mixture fraction is within flammability limits must exist : combustion occurs between the fuel vapour radially dispersed by the swirl and the ambient air, where the equivalence ratio is low enough
3. the heat release must be high enough to maintain evaporation and reaction : the sum of heat flux Π and heat release $\dot{\omega}_T$, plotted on Fig. 9, allows to identify the zone (—) where the heat transfer due to evaporation extinguishes the flame : $\Pi + \dot{\omega}_T = 0$.

In the present case, the flame front is stabilised by the CRZ (1.) but the heat release magnitude is reduced in the evaporation zone because of both effects (2.) and (3.). To determine the flame regime (premixed and/or diffusion), the Takeno index $\mathcal{T} = \nabla Y_F . \nabla Y_O$ and an indexed reaction rate $\dot{\omega}_F^* = \dot{\omega}_F \frac{\mathcal{T}}{|\nabla Y_F| . |\nabla Y_O|}$ are used. The flame structure is then divided into two parts : $\dot{\omega}_F^* = +\dot{\omega}_F$ in the premixed regime part and $\dot{\omega}_F^* = -\dot{\omega}_F$ in the diffusion regime part (Fig. 10). In the primary zone, the partially premixed regime is preponderant because of the unsteady inhomogeneous fuel vapour. In the dilution zone, the unburned fuel reacts with dilution jets through a diffusion flame, as confirmed by the coincidence between the flame and the stoichiometric line.

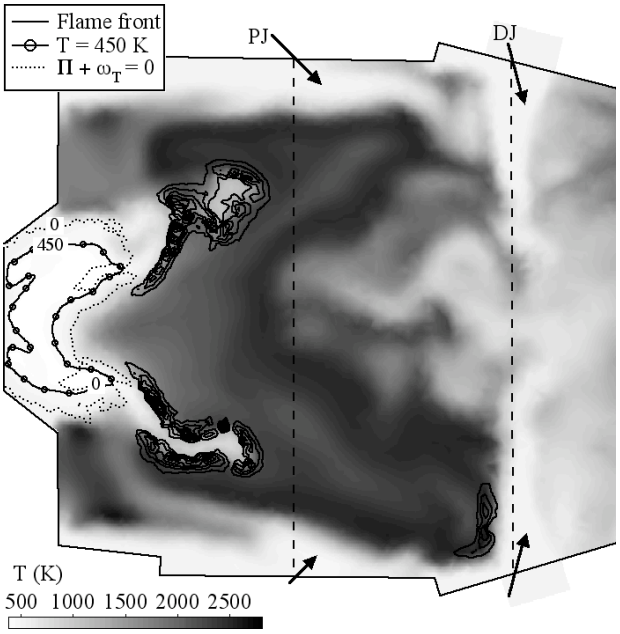

Fig. 9 Flame front

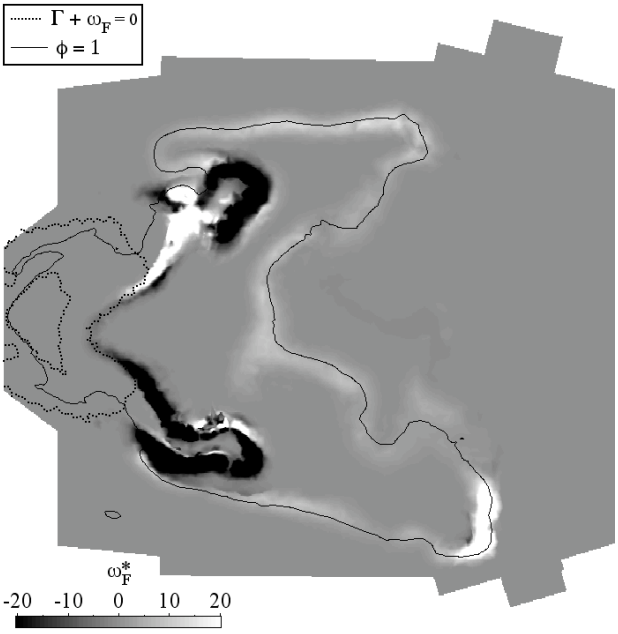

Fig. 10 Flame structure

PVC influence

The PVC, defined on Fig. 11a, controls the motions of both the vaporised fuel VF and the flame front. The cut plane, defined on Fig. 11a, is presented on Fig. 11b with the temperature field, the maximum fuel mass fraction (white lines) and the flame front (black isolines of reaction rate $\dot{\omega}_F$). The CRZ stabilises hot gases and enhance evaporation leading to a cold annular zone where the maximum fuel mass fraction precesses. The flame motion follows the PVC and the reaction rate is driven by the fuel vapour concentration.

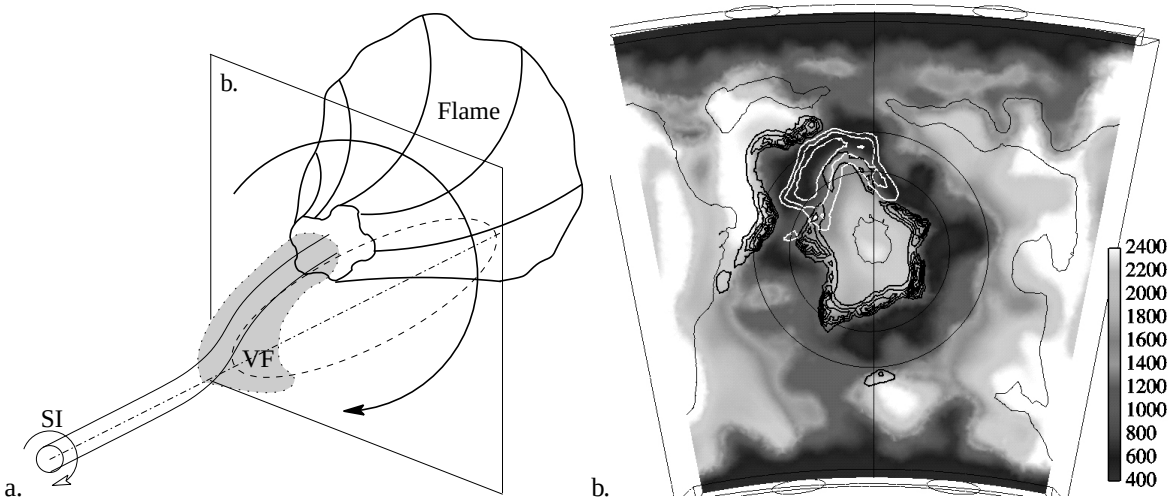

Fig. 11 PVC influence on evaporation and combustion

Ignition sequence

Spark-like numerical method

The numerical method used to mimic an ignition by spark plug in the combustion chamber is the addition of the source term $\dot{\omega}_{spark}$ in Eq. (4). This source term, defined by Eq. (7), is a gaussian function located at (x_0, y_0, z_0) near the upper wall between both primary jets and deposited at $t = t_0 = 0$. The ignition delay, typical of industrial spark plugs, is $\sigma_t = 0.16\ ms$.

$$\dot{\omega}_{spark} = \frac{E_{spark}}{(2\pi)^2 {\sigma_t}{\sigma_r}^3} e^{-\frac{1}{2}\left[\left(\frac{t-t_0}{\sigma_t}\right)^2+\left(\frac{x-x_0}{\sigma_r}\right)^2+\left(\frac{y-y_0}{\sigma_r}\right)^2+\left(\frac{z-z_0}{\sigma_r}\right)^2\right]} \tag{7}$$

Temporal evolution

The temporal evolution of the spark ignition is presented on Fig. 12 where the source term $\dot{\omega}_{spark}$, the maximum heat release $\dot{\omega}_T$ and the maximum temperature are plotted. First, the maximum temperature rises smoothly because of the source term on energy equation. When this temperature is sufficient, the reaction occurs between fuel vapour and air leading to a sudden increase of the heat release of the exothermic reaction and then, the maximum temperature rapidly rises. Once the source term is over, the maximum heat release decreases. The maximum temperature corresponds to the hot gases : the ignition is successful.

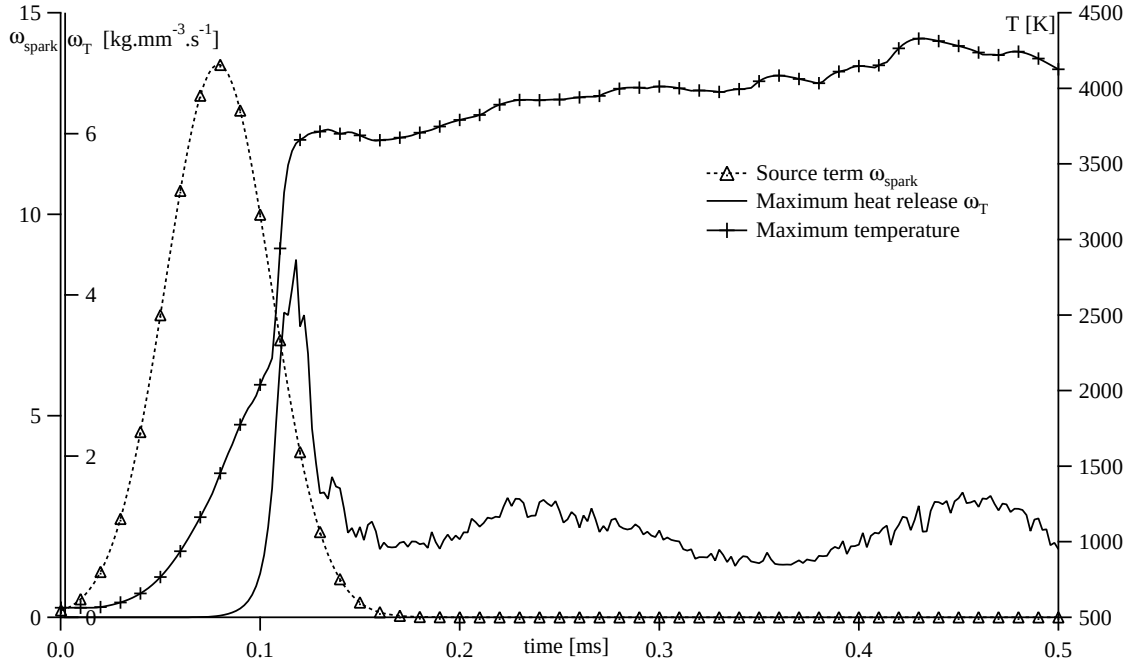

Fig. 12 Source term $\dot{\omega}_{spark}$, maximum heat release $\dot{\omega}_T$, maximum temperature

The sequence of ignition is illustrated on the longitudinal central cut plane on Fig. 13 with the fuel mass fraction field and the reaction rate isolines, where the first image is presented at $t = 0.2\ ms$ and after, successive images are separated by $\Delta t = 0.2\ ms$. At the beginning of the computation, the $15\ \mu m$ droplets evaporate in the ambient air at $T = 525\ K$ creating a turbulent cloud of vaporised fuel in the whole primary zone. This fuel vapour distribution, whose stabilisation is ensured by the CRZ, propagates from the evaporation zone to the spark plug area. At $t = 0$, the spark ignition occurs leatding to the creation of a hot kernel. The propagation of the flame front created by this pocket of hot gases is highly controlled by the fuel vapour distribution between $t = 0$ and $t = 1\ ms$. Once the flame front reaches the CRZ ($t \simeq 1\ ms$), there is no more vaporised fuel and the flame must evaporate the fuel droplets leading to an increase of the maximum fuel mass fraction in the CRZ. This evaporation process stabilise the flame front as explained in the previous section on steady spray flame.

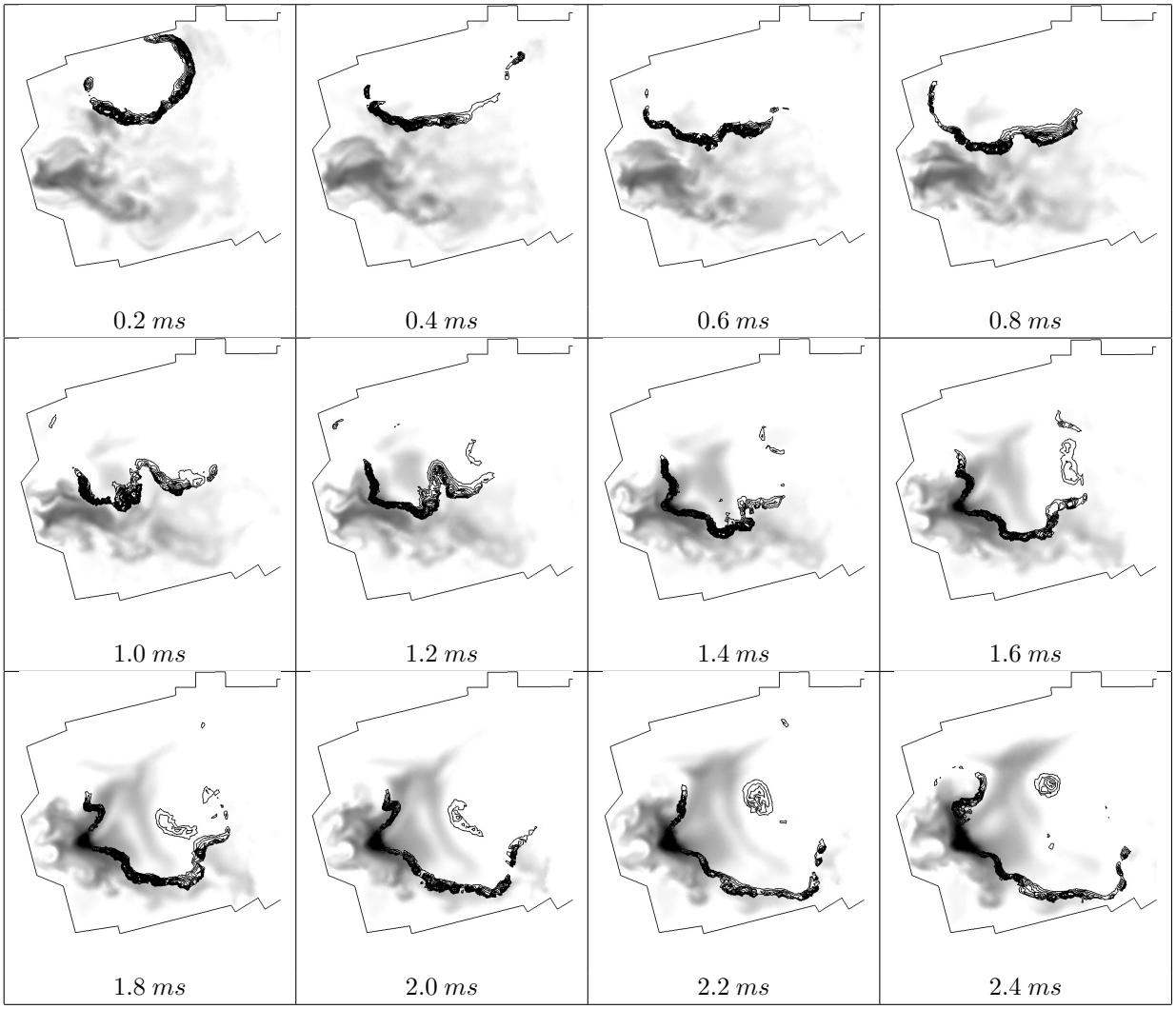

Fig. 13 Flame front propagation on fuel mass fraction field (white : 0 → black : 0.35)

Conclusions

A steady spray flame in a realistic aeronautical combustor has been computed using the parallel LES Euler/Euler solver AVBP. The influence of the dispersed phase on the flame motion has been highlighted, in particular the role of the evaporation process. The unsteady approach brings totally new insight into the physics of such complex reactive two-phase flows. Furthermore, it allows the computation of an ignition sequence from the formation of the first spherical flame front to the stabilisation of the turbulent spray flame. To conclude, the LES technique is a powerful tool to mimic ignition sequences and understand turbulent spray flame structure in realistic combustors.

References

[1]P.E. Desjardins and S.H. Frankel. Two dimensional large eddy simulation of soot formation in the near field of a strongly radiating nonpremixed acetylene-air jet flame. *Combust. Flame* , 119(1/2):121–133, 1999.

[2]O. Colin. *Simulation aux Grandes Echelles de la Combustion Turbulente Prémélangée dans les Statoréacteurs*. PhD thesis, INP Toulouse, 2000.

[3]C. Angelberger, F. Egolfopoulos, and D. Veynante. Large eddy simulations of chemical and acoustic effects on combustion instabilities. *Flow Turb. and Combustion* , 65(2):205–22, 2000.

[4]H. Pitsch and L. Duchamp de la Geneste. Large eddy simulation of premixed turbulent combustion using a level-set approach. *Proceedings of the Combustion Institute*, 29:in press, 2002.

[5]C.D. Pierce and P. Moin. Progress-variable approach for large eddy simulation of non-premixed turbulent combustion. *J. Fluid Mech.* , 504:73–97, 2004.

[6]L. Selle. *Simulation aux grandes échelles des couplages acoustique / combustion dans les turbines á gaz*. Phd thesis, INP Toulouse, 2004.

[7]K. Mahesh, G. Constantinescu, S. Apte, G. Iaccarino, F. Ham, and P. Moin. Progress towards large-eddy simulation of turbulent reacting and non-reacting flows in complex geometries. In *Annual Research Briefs*, pages 115–142. Center for Turbulence Research, NASA Ames/Stanford Univ., 2002.

[8]K. Mahesh, G. Constantinescu, and P. Moin. A numerical method for large-eddy simulation in complex geometries. *J. Comput. Phys.* , 197:215–240, 2004.

[9]S. V. Apte, M. Gorokhovski, and P. Moin. Large-eddy simulation of atomizing spray with stochastic modeling of secondary breakup. In *ASME Turbo Expo 2003 - Power for Land, Sea and Air*, Atlanta, Georgia, USA, 2003.

[10]F. Ham, S. V. Apte, G. Iaccarino, X. Wu, M. Herrmann, G. Constantinescu, K. Mahesh, and P. Moin. Unstructured les of reacting multiphase flows in realistic gas turbine combustors. In *Annual Research Briefs - Center for Turbulence Research*, 2003.

[11]R.V.R. Pandya and F. Mashayek. Two-fluid large-eddy simulation approach for particle-laden turbulent flows. *Int. J. of Heat and Mass transfer*, 45:4753–4759, 2002.

[12]E. Riber, M. Moreau, O. Simonin, and B. Cuenot. Towards large eddy simulation of non-homogeneous particle laden turbulent gas flows using euler-euler approach. In *11th Workshop on Two-Phase Flow Predictions*, Merseburg, Germany, 2005.

[13]M. García, Y. Sommerer, T. Schönfeld, and T. Poinsot. Evaluation of euler/euler and euler/lagrange strategies for large eddy simulations of turbulent reacting flows. In *ECCOMAS Thematic Conference on Computational Combustion*, 2005.

[14]H. Pitsch and N. Peters. A consistent flamelet formulation for non-premixed combustion considering differential diffusion effects. *Combust. Flame* , 114:26–40, 1998.

[15]L. Selle, G. Lartigue, T. Poinsot, P. Kaufman, W. Krebs, and D. Veynante. Large eddy simulation of turbulent combustion for gas turbines with reduced chemistry. In *Proceedings of the Summer Program - Center for Turbulence Research*, pages 333–344, 2002.

[16]R. Borghi. Background on droplets and sprays. In *Combustion and turbulence in two phase flows, Lecture Series 1996-02*. Von Karman Institute for Fluid Dynamics, 1996.

[17]O. Delabroy, F. Lacas, B. Labegorre, and J-M. Samaniego. Paramètres de similitude pour la combustion diphasique. *Revue Générale de Thermique*, (37):934–953, 1998.

[18]J. Réveillon, M. Massot, and C. Pera. Analysis and modeling of the dispersion of vaporizing polydispersed sprays in turbulent flows. In *Proceedings of the Summer Program 2002 - Center for Turbulence Research*, 2002.

[19]R.D. Reitz and R. Diwakar. Structure of high pressure fuel sprays. Technical Report Tech. Rep. 870598, SAE Technical Paper, 1987.

[20]J.-Ph. Légier, T. Poinsot, and D. Veynante. Dynamically thickened flame large eddy simulation model for premixed and non-premixed turbulent combustion. In *Summer Program 2000*, pages 157–168, Center for Turbulence Research, Stanford, USA, 2000.

[21]O. Colin, F. Ducros, D. Veynante, and T. Poinsot. A thickened flame model for large eddy simulations of turbulent premixed combustion. *Phys. Fluids* , 12(7):1843–1863, 2000.

[22]F. Nicoud and F. Ducros. Subgrid-scale stress modelling based on the square of the velocity gradient. *Flow Turb. and Combustion* , 62(3):183–200, 1999.

[23]T. Poinsot and D. Veynante. *Theoretical and numerical combustion, second edition*. R.T. Edwards, 2005.

[24]C. Hirsch. *Numerical Computation of Internal and External Flows*. John Wiley & Sons, 1989.

[25]T. Poinsot and S. Lele. Boundary conditions for direct simulations of compressible viscous flows. *J. Comput. Phys.* , 101(1):104–129, 1992.

[26]L. Selle, F. Nicoud, and T. Poinsot. The actual impedance of non-reflecting boundary conditions: implications for the computation of resonators. *AIAA Journal* , 42(5):958–964, 2004.

[27]C. Martin. Eporck user guide v1.8. Technical report, CERFACS, 2004.

[28]S. C. Li, B. Varatharajan, and F. A. Williams. The chemistry of jp-10 ignition. *AIAA*, 39(12):2351–2356, 2001.

[29]O. Lucca-Negro and T. O'Doherty. Vortex breakdown: a review. *Prog. Energy Comb. Sci.* , 27:431–481, 2001.

[30]L. Selle, G. Lartigue, T. Poinsot, R. Koch, K.-U. Schildmacher, W. Krebs, B. Prade, P. Kaufmann, and D. Veynante. Compressible large-eddy simulation of turbulent combustion in complex geometry on unstructured meshes. *Combust. Flame* , 137(4):489–505, 2004.